

Electronic interactions of medium-energy ions in hafnium dioxide

D. Primetzhofer*

Ion Physics, Department of Physics and Astronomy, Uppsala Universitet, Box 516, S-751 20 Uppsala, Sweden

(Received 14 February 2014; published 20 March 2014)

In this article, the electronic interaction of medium-energy ions with hafnium dioxide is studied. Stopping cross sections for He ions in the energy range from 30 to 160 keV have been measured in backscattering experiments from thin films of HfO₂ on Si using time-of-flight medium-energy ion scattering. The observed energy loss for helium ions is found to be high compared to expectations from earlier results for hydrogen in HfO₂, a result which indicates a contribution from energy-loss processes that is different from direct excitation of electron-hole pairs in close collisions. Furthermore, data exhibit a significant deviation from velocity proportionality. A discussion of the results, together with data from studies for H and He in SiO₂, show characteristic differences which are traced back to different electronic structures of the target materials and their influence on the charge-exchange channels that are active in the interaction with helium. Charge exchange, in turn, via shifted mean-charge states, will influence the observed ionization along the ion track. The results can furthermore serve as reference values for ion-beam-based depth profiling at medium and low ion energies.

DOI: [10.1103/PhysRevA.89.032711](https://doi.org/10.1103/PhysRevA.89.032711)

PACS number(s): 79.20.Rf, 34.50.Fa, 34.50.Bw

I. INTRODUCTION

The processes which lead to the exchange of energy between a moving ion and the electronic system of the material it traverses are both of fundamental interest and of utmost importance for ion-beam-based depth profiling techniques of thin films as well as ion-beam-based material modification. These reasons have led to many experimental and theoretical investigations of the associated phenomena in the regime of MeV ion energies as they are commonly employed in conventional ion-beam analysis (IBA).

In consequence of the ongoing miniaturization in electronics, sensor technology, etc., new ion-beam-based tools which employ lower ion energies are being developed in an effort to overcome the limited depth resolution of conventional IBA. Methods such as medium-energy ion scattering (MEIS) or high-resolution Rutherford backscattering spectrometry (HR-RBS) make use of magnetic and electrostatic spectrometers (see, e.g., Refs. [1,2]) as well as modified solid-state detectors [3] with an improved energy resolution δE . Consequently, the higher relative energy loss $\Delta E/E_0$ per unit path length can be exploited in such experiments. It has been shown that monolayer resolution can be obtained under certain conditions by these methods [4,5]. Of course these approaches have also generated a demand for a quantification of the ion energy loss and the associated mechanisms at the associated ion energies.

The quantity of interest in such investigations, having a dimension of a force dE/dx , i.e., the mean energy loss per unit path length, is referred to as the stopping power S of the material for a certain ion species [6]. An alternative and often more convenient expression is the electronic stopping cross section ε defined by $1/n dE/dx$, where n is the atomic number density; by this definition the target density does not play any significant role.

At sufficiently high energies the projectiles are unable to bind electrons, a fact that simplifies the modeling of energy

loss. The description becomes more complicated towards lower ion energies as ions will be only partially stripped, and thus a model for the effective charge is necessary to describe the observed energy loss [7]. The difference in ionization along the ion track for different charge states of the penetrating ion, together with the energy dependence of cross sections and the maximum energy transfer in the collisions between ion and target electrons, lead to the observation of a pronounced maximum at an energy that depends on the ion species (e.g., around 100 keV for protons [8]).

Despite these complications different models permit a good qualitative and quantitative prediction of S for almost any compound [9–15], down to energies around the stopping-power maximum, and large compilations of experimental and theoretical data for many different materials are available [16]. These compilations, however, also illustrate the increased uncertainty or complete lack of both experimental and theoretical data towards lower energies.

At energies below the stopping maximum the simplest reasonable model system to describe the energy loss to the electronic system is an ion that moves in a free-electron gas (FEG). This approach results typically in velocity proportional stopping power [17], with a proportionality coefficient Q that depends on the atomic number of the projectile and the electron gas density n_e . In this context it is common to express density via the Wigner-Seitz radius of the electron gas $r_s = (3/4\pi n_e)^{1/3}$.

Indeed, many investigated systems have been found to show this behavior; for metals with occupied electronic states up to the Fermi level E_F and unoccupied states available directly above E_F this can be also well understood. Due to the excitation thresholds of certain electronic states and the limited maximum energy transfer in a binary collision, pronounced deviations have been found at sufficiently low energies, i.e., below 10 keV for protons or ~ 25 keV for He ions, for some noble metals and semiconducting and insulating materials [18–23].

At energies of about 1 a.u. and for hydrogen ions, however, in most systems velocity proportional stopping was observed

*daniel.primetzhofer@physics.uu.se.at

[24–26], with the only exception being protons in He [27]. Nevertheless, the observed magnitude of electronic stopping in compounds was, in certain cases, found to be strongly affected by the chemical composition also up to energies of about 100 keV [28,29].

The energy loss of He ions is of particular fundamental interest, since its electronic structure enables energy dissipative charge-exchange processes not observed for hydrogen projectiles [30]. Both changed mean charge states as well as a direct energy loss in the process are possible consequences. These charge-exchange processes can explain the mentioned deviation for the velocity proportionality of protons in He [27] and have also been proposed to be responsible for deviations from $S \sim v$ of He in Al [31] as well as for He in Au and Pt at energies around 60 keV [32]. The underlying processes are well investigated, especially at very low ion energies as employed in low-energy ion scattering, and are found to exhibit a strong dependence on the electronic structure of target atoms [33]. In combination with O atoms in the target, a further complication of the situation is expected since oxygen has been found to significantly influence the above-mentioned charge-exchange processes in many oxide systems [33,34].

For these reasons, HfO₂, which is an insulating oxide with a band gap of about 6 eV and with distinct electronic states due to the 4*f* electrons of Hf forming a narrow subband around −17 eV and the oxygen 2*p* electrons around −5 eV [35,36], is of particular interest for an investigation of the electronic interactions of medium-energy He ions. A previous investigation found no clear influence of the samples' complicated electronic structure on the electronic energy loss of hydrogen in HfO₂ and resulted in excellent velocity proportionality of *S* observable down to ion energies of 5 keV, i.e., ~0.45 a.u. in the ion velocity [37].

For a couple of years stacks containing HfO₂ have been used as gate dielectric layer, replacing SiO₂ in state-of-the-art metal-oxide-semiconductor field-effect transistors (MOSFET). The miniaturization of these devices is a continuing process and HfO₂ additionally acts as a model systems for similar high-*k* material stacks. Consequently, numerous studies which employ medium-energy ion scattering (MEIS) to characterize stacks of high-*k* materials such as HfO₂ have been published [38–41].

Thus, besides the fundamental interest, accurate reference stopping powers for He ions in high-*k* compounds are also of relevance for obtaining correct depth scales in ion-beam-based analyses of the above-mentioned systems. Interestingly, to the best of our knowledge, only one study of electronic energy loss dedicated to H and He in HfO₂ has been published [42] at energies around the stopping maximum. For He and at energies where typical MEIS studies are conducted, i.e., 100 keV, for which the influence of the less adiabatic character of the interaction of the ions with the targets' electronic systems is expected to become more prominent, only extrapolations and calculations have been found at present.

II. EXPERIMENT AND EVALUATION

Sample manufacturing was done *ex situ* under clean room conditions. All depositions were done on *p*-type Si(100) substrates cleaned by H₂SO₄:H₂O and HF5%. The SiO₂

buffer layers were grown via O₃ oxidization. The HfO₂ is deposited by atomic layer deposition (ALD). Ellipsometry measurements yielded nominal thicknesses in the range of 1.3–12.8 nm for different films. Calibration experiments using Rutherford backscattering spectrometry (RBS) were performed employing a 5 MV 15SDH-2 tandem accelerator at the Ångström Laboratory at Uppsala University. Backscattering spectra were recorded for 2 MeV He⁺ ions to obtain the areal thickness of the HfO₂ films in atoms/cm². Additional measurements with well-known non-Rutherford cross sections around 3.03 MeV He⁺ [43] for enhancement of the O signal yielded excellent film stoichiometry.

A film with calibrated thicknesses of 12.2 nm, assuming a bulk density of HfO₂, was employed for energy-loss measurements, with additional control measurements on films down to a calibrated thickness of 1.8 nm [44]. The energy-loss experiments were performed with the time-of-flight MEIS (TOF-MEIS) setup at Uppsala University [45]. A large solid-angle microchannel-plate (MCP) detector (the diameter of the active area was 120 mm at a distance of 300 mm, which results in a ~0.12 sr solid angle) which can be rotated around the sample permits one to record position-sensitive time spectra for different scattering angles in backscattering geometry. In the present experiment scattering angles of 135° and 120° have been employed. Due to the large area of the detector, the particle flux can be kept extremely low (on the order of 10 nC per spectrum), which thus enables measurements without any significant sample damage due to, e.g., sputtering.

He⁺ ions with primary energies E_0 between 30 and 160 keV were used to obtain the presented stopping-power data. The energy resolution obtainable in the experiments corresponds to the time resolution achieved in a combination of the beam chopper and the detection system as well as an inevitable energy spread from the ion source. In the present experiment, energy resolutions were typically found between 1 and 3 keV, with the highest values at the highest energies. Higher resolutions are achievable [44], however, they linked with a substantial increase in measurement time.

While the whole detector was sensitive for particles during experiments, only a selected region, i.e., an angular interval of 1°–2° around the scattering angle for the detector center, was selected for evaluation. For scattering of He from hafnium this selection introduces a geometrical straggling contribution of at most 0.2% of E_0 . Since experiments were conducted under normal incidence, the above-mentioned angular interval corresponds to a curved shape on the detector, making use of different azimuth scattering directions with equivalent scattering geometry. The effective solid angle of the detector used is thus found to be between 11% and 22% of the total solid angle, resulting in ~13 to ~26 msr. Note that small differences in sample-detector distance result (<2%) for different trajectories as a consequence of the planar detector surface. These differences are considered accordingly when the TOF data are transformed to energy spectra. An example for an energy-converted TOF-MEIS spectrum for 60 keV He⁺ is shown in Fig. 1. The dominant feature in the figure is due to backscattering from Hf in the HfO₂ film. Thus, since the spectra still resemble typical RBS data for thin films, the width of the spectrum is a direct measure for the thickness of the film and the magnitude of the energy loss with only some influence

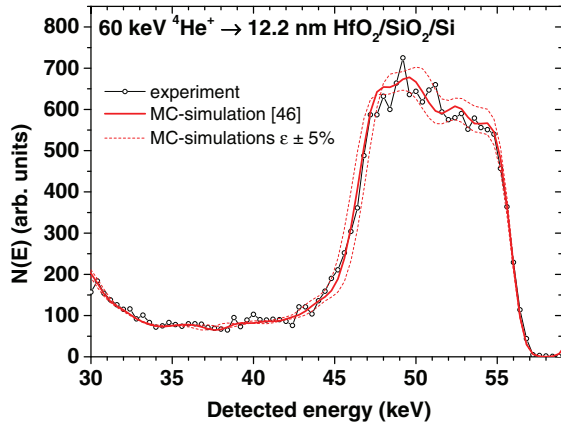


FIG. 1. (Color online) Energy-converted TOF-MEIS spectrum for scattering of 60 keV $^4\text{He}^+$ from a 12.2-nm HfO_2 film and a scattering angle of 120° (open symbols). Also shown are Monte Carlo simulations obtained with the TRBS simulation code (red solid and dashed lines) [46]. For details, see text.

of multiple scattering being noticeable in a low-energy tail. The total energy-loss straggling is apparently found to be low compared to the energy loss, with the shape of the high- and low-energy edge of the spectrum being dominated by the limited energy resolution of the detection system.

To obtain quantitative information on electronic energy loss, the backscattered yield for a given scattering angle is simulated by Monte Carlo (MC) trajectory calculations by the TRBS code (trim for backscattering) [46] (red solid and dashed lines in Fig. 1). In the simulations different interatomic potentials with adjustable screening [Ziegler-Biersack-Littmark (ZBL) and Thomas-Fermi-Molière (TFM) [47,48]] are available. The electronic energy loss is modeled according to Ref. [47]. The electronic energy-loss straggling can be modeled according to Chu [49] for both protons and helium. The electronic energy loss used in the simulations can be tuned by a constant scaling factor (see the different solid and dashed lines in Fig. 1). For a fixed thickness of the HfO_2 layer this factor is adjusted until the width of the feature from backscattering from Hf is matched. The simulated spectra are additionally convoluted with a Gaussian to account for the energy resolution of the experiment, which then results in excellent fits for the whole low-energy edge instead of an equivalent width at the half-height. The presented evaluation procedure thus finally results in a single value for the stopping power employed in the simulations at the incident velocity for each spectrum analyzed. For thin targets with $\Delta E \ll E_0$ this methodology permits an accurate evaluation of the electronic energy loss the detected ions have experienced, which is virtually independent of the stopping model in the program. In the present study the mean ion energy was always found to be more than 85% of E_0 and the overall energy loss for single scattered particles never exceeded 25% of the primary energy. Furthermore, some previous studies with a similar methodology have resulted in a nonlinear velocity scaling of ϵ that is different from the modeling in the program and that was in excellent agreement with other results obtained in transmission (compare, for example, Refs. [19] and [20] as well as Refs. [22] and [23]). It should be also noted that the

program excellently reproduces contributions from multiple scattering, as can be seen from the fit to the background towards lower energies. This guarantees that the small but present contributions from nuclear stopping are handled appropriately and do not enter the deduced electronic stopping cross sections.

The uncertainty of the deduced stopping cross sections is influenced by different factors. One prominent source of systematic errors is the thickness calibration by RBS, where the substrate signal serves as the normalization and the employed energy loss and other sources of systematic errors in simulation and measurement of the Si signal inevitably enter the evaluation of the Hf concentration. From scattering of the available stopping data [16], inaccuracies in the stopping power of He in Si might introduce a possible systematic error of, in principle, up to 2.5% into the obtained results. Note, however, that the employed stopping power in Si in the present study has been claimed to be correct to within 0.6% [50]. Due to this high precision in the used stopping power, other procedures using reference samples were not expected to result in a superior thickness calibration. Another important potential source of errors can be found in channeling in the Si substrate. Several measurements for small changes in sample orientation were performed to eliminate this error. Nevertheless, it is very difficult to ensure a geometry which yields a signal as expected from an amorphous sample. To account for these uncertainties, the total systematic errors from the thickness calibration are fixed to 2.5% for the present investigation. Counting statistics, together with the accuracy of the fitting procedure to the leading and the trailing edge of the experimental spectra, can lead to errors, which are, for the present data, estimated to be 3% (see Fig. 1, which shows ϵ modified by $\pm 5\%$ for comparison). Finally, in stopping experiments for compound materials, additionally, the influence of the film stoichiometry has to be taken into account. Nonstoichiometric films and a fit to the signal from scattering from Hf and Si exclusively could lead to wrong stopping cross sections, if the investigated compound deviates from the expected composition. Since the growth of HfO_2 layers is a standard process [51] and the joint results from ellipsometry, capacitance measurements, and ion scattering suggest excellent film stoichiometry, a possible systematic error of at most 5% may be attributed to this issue. Thus, the cumulative error of the deduced stopping cross sections is expected not to exceed 7%. Note that the systematic uncertainties, if present, would mainly introduce a scaling factor, i.e., the velocity and energy scaling of obtained stopping cross sections would remain unaffected.

III. RESULTS AND DISCUSSION

Electronic stopping cross sections ϵ were deduced for ^4He at primary ion energies between 30 and 160 keV, which corresponds to velocities of 0.55–1.26 a.u. In Fig. 2 we present the obtained stopping cross sections ϵ as functions of the ion energy (red asterisks). The error bars depicted for all data points represent the statistical error, with additional wider error bars shown for the highest and lowest energy, which show how the cumulative errors are dominated by possible systematic contributions. Also shown are data obtained in a previous experiment by Behar *et al.* [42] (open asterisks) as well as theoretical predictions made in the same work based on the

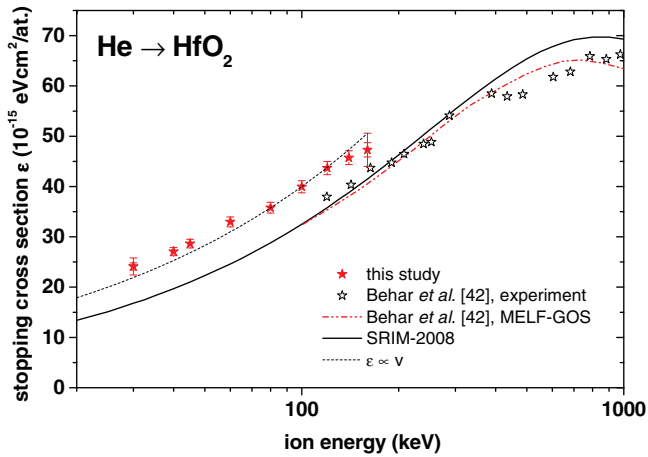


FIG. 2. (Color online) Electronic stopping cross sections of ^4He ions in HfO_2 presented as a function of the ion energy (red solid asterisks). Data are found to deviate to higher values compared to predictions from theory at lower energies. Other experimental data (open asterisks) and calculations from Behar *et al.* [42] (red dashed line) as well as SRIM predictions (solid line) are included in the figure. For details, see text.

Mermin energy-loss function–generalized oscillator strength (MELF-GOS) model [52,53] (red dashed-dotted line). Data from Behar *et al.* show a trend to deviate from stopping and range of ions in matter (SRIM) predictions (black solid line) and the MELF-GOS modeling towards higher values when decreasing the ion energy. These He data show a very similar behavior, with an equal slope for the region where data overlap. For comparison, the black dashed line through the present data indicates a velocity proportional behavior of electronic stopping with an adjusted proportionality coefficient. To discuss these effects in more detail, the same experimental data are plotted in Fig. 3 as functions of the ion velocity. Additionally, the figure also holds data for hydrogen ions in HfO_2 [37] as well as data for H and He ions in SiO_2 [23,54–57].

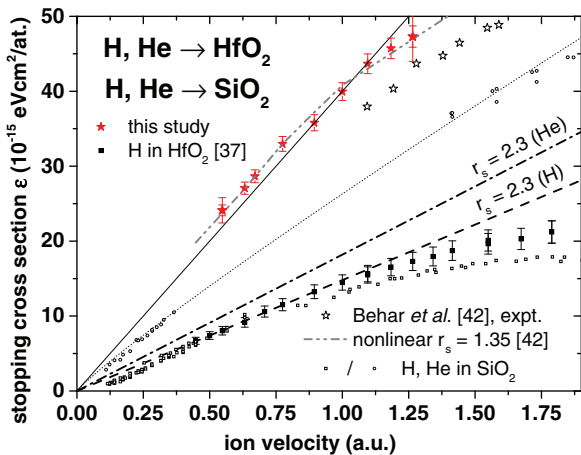


FIG. 3. (Color online) Electronic stopping cross sections for ^4He (same data as in Fig. 2) and H [37] in HfO_2 as a function of the ion velocity. Also shown are data and calculations from Behar *et al.* [42]. For comparison, data for H and ^4He in SiO_2 [23,54–57] are also shown as open squares and open circles. For details, see text.

Note that data for hydrogen in hafnium oxide are found to exhibit excellent velocity proportionality at velocities below 1 a.u.

As stated in the Introduction, a free-electron gas model can be used as a starting point for the interpretation of the observed data [58]. For the hydrogen data such a comparison revealed an effective electron density of $3.7e^-$ per molecule contributing to electronic stopping [37]. This is equivalent to an r_s value, i.e., the radius of the spherical volume occupied, of one electron in the FEG to be 2.5 a.u. When the observed stopping cross section for ^4He ions in HfO_2 at 1 a.u. in the ion velocity is used for such a comparison within the same set of density functional theory (DFT) calculations, it is found that the resulting r_s value is only about 1.75 a.u. In terms of an effective electron density this would correspond to more than $11e^-$ contributing to the electronic stopping in the case of He, if the energy-loss processes were due to the creation of electron-hole pairs exclusively, i.e., three times more electrons participating in the energy-loss processes. Note that, depending on details in the modeling, DFT approaches can also yield slightly different values for the density parameter [59]. In fact, the modeling from the latter group results in a value of $r_s = 1.62$ for He whereas hydrogen data agree well with $r_s = 2.3$ (see the dashed line in Fig. 3). A more complex nonlinear modeling by Behar *et al.* for He results in perfect agreement with the observed data for an r_s value of 1.35 in the case of He (data extracted from Ref. [42]). As a matter of fact, in any approach there remains a significant discrepancy in electron density necessary to explain the magnitude of the energy loss observed for He ions and hydrogen (see the dashed and dashed-dotted line in Fig. 3). Even if free-electron models are of course not perfectly applicable to insulating materials, the observed difference can be considered as a strong indication that the observed energy loss of He ions cannot be completely described by the very same mechanisms as for hydrogen, i.e., binary collisions exciting electron-hole pairs.

In the following we want to compare the observed behavior to what has been observed for H and He in SiO_2 . The system of SiO_2 is an oxide of similar chemistry, with, however, some significant differences in the density of states [60,61], e.g., it features an even larger band gap than HfO_2 and f states are absent. In any case, the energy loss of hydrogen projectiles is found to be of equal magnitude for both HfO_2 and SiO_2 at velocities between 0.4 and 0.8 a.u. The increasing discrepancies towards higher energies probably can be attributed to beginning excitation of f states found at -16 eV with respect to the valence-band edge in hafnium oxide which increases the effective electron density [35]. Towards lower energies, and thus decreasing energy transfers, the density of states becomes dominated by lone-pair states of O $2p$ character which should be identical for both compounds and thus should equally contribute to the energy loss [35,61]. Only at very low energies does the large band gap of SiO_2 lead to an apparent threshold in electronic stopping.

When comparing data for He for HfO_2 and SiO_2 it becomes obvious that, different from the observations for hydrogen, an interpolation of available data (dotted line) predicts a significantly (25%–40%) lower electronic stopping power in SiO_2 than that observed in HfO_2 for equal velocities. This would result in a more equal number of electrons contributing

to energy loss in the case of SiO_2 in a free-electron model—but also for SiO_2 a discrepancy remains. This result can be interpreted possibly as a weaker contribution of the energy-loss mechanism that is different from direct electron-hole pair creation in binary collisions for He in SiO_2 as compared to HfO_2 .

These observations are in accordance with several other recent experiments which gave an indication that additional energy-loss channels in He indeed are likely and may be linked to charge-state fluctuations of the He projectile [31,32]. These charge-exchange processes, in turn, are mediated by an interaction with the target atom core levels [33]. In particular, levels which are found almost in resonance with the unperturbed He $1s$ level are found to strongly influence charge-exchange processes in low-energy ion scattering, e.g., in Ge d states are known to lead to oscillatory ion yields [62]. As stated in the Introduction, oxygen is also known for its strong influence on charge-exchange processes in low-energy ion scattering, which can be attributed to the presence of the $2s$ level typically found below -15 eV with respect to the valence-band edge in oxides. A possible strong interaction with these states can explain the increased energy loss for He ions by two cumulative effects: first, a change, i.e., an increase in the mean charge state and thus increasing ionization, and second, directly by the dissipative nature of the charge-exchange cycles for He ions. When comparing Si and Hf, for Hf additionally heavily populated f states are found at similar binding energies which can explain the observed discrepancies between HfO_2 and SiO_2 . Since the probability for such processes is expected to show a different energy dependence, it could also yield an explanation for the observed change in slope of the stopping cross section. Figure 4 shows the magnitude of the observed effect by plotting the stopping-power data normalized by the ion velocity, i.e., the proportionality coefficient to velocity. A monotonous increase towards lower energies is observed. The error bars given represent statistical errors only, since

systematical errors would only lead to a parallel shift of the present data in Fig. 4. An increase in the friction coefficient can be interpreted in this picture as an increasing fraction of the electronic energy loss being governed by processes not included in the modeling for a free-electron gas. A change in the number of electrons participating in energy-loss processes in binary collisions would, in contrast, typically lead to a decrease in the friction coefficient, since decreasing energy can eventually make it impossible to excite certain states which correspond to a decrease in the number of participating electrons (see the Introduction).

Note that also for SiO_2 the energy loss of He ions showed a possibly related peculiarity at very low velocities [23]. Whereas electronic stopping for hydrogen apparently vanished, in accordance with expectations due to the density of states, for ^4He extrapolation from the data indicated that certain energy-loss mechanisms still appear to be active (see the low velocities in Fig. 3).

In total, the present comparison of systems thus indicates the possible importance of electronic processes in the projectile system triggered by localized states in the electronic system of the target which are, however, not themselves directly excited.

IV. SUMMARY AND CONCLUSIONS

In this article, experimentally deduced stopping cross-section data for He in hafnium oxide are presented. A detailed discussion of the obtained results in comparison with previous data for hydrogen in HfO_2 and with data for SiO_2 is made. The analysis reveals that data for helium exhibit a systematically high stopping power in contrast to expectations when similar interaction mechanisms, i.e., excitation of target electrons in binary collisions, are assumed.

Also, a deviation from the expected velocity scaling of the observed energy loss is found. A common qualitative explanation for the magnitude and energy and velocity scaling of all data is proposed based on the influence of deeper lying electronic orbitals, i.e., O $2s$ as well as Hf $4f$ states, which cannot be directly excited but, due to their interaction with the electronic system of the He ion, can lead to more complex energy-loss processes which cannot take place in the interaction with hydrogen.

To check for the accuracy of the present explanations, a thorough theoretical analysis of the influence of tightly bound electronic states would be of great relevance. Also, a different experimental approach, probing the possible impact parameter dependencies of these energy-loss channels, i.e., a comparison with transmission experiments at medium and low energies, could advance understanding. Finally, a thorough investigation of charge-exchange processes between He ions and Hf, but also for oxides in general, would yield complementary information.

ACKNOWLEDGMENT

The author expresses his gratitude to E. Dentoni Litta and A. Hallén, who provided the hafnium oxide samples used in this work, and to Ch. Zoller for support with the non-Rutherford backscattering experiments on HfO_2 .

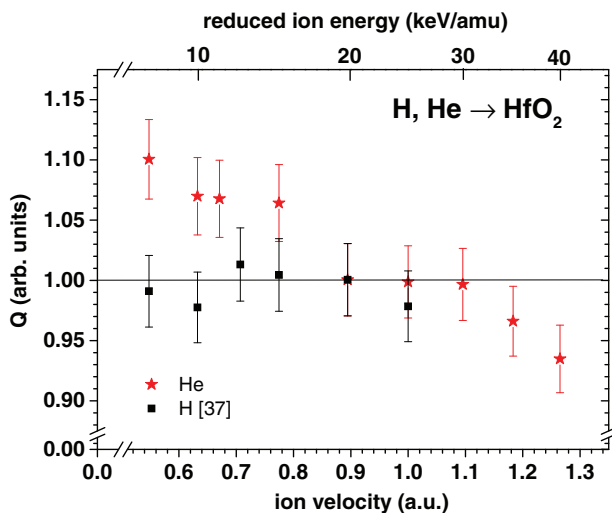


FIG. 4. (Color online) Proportionality coefficients Q deduced from stopping cross sections normalized for the ion velocity for H and He as derived in Ref. [37] and the present study (black squares and red asterisks, respectively).

- [1] J. Vrijmoeth, P. M. Zagwijn, J. W. M. Frenken, and J. F. van der Veen, *Phys. Rev. Lett.* **67**, 1134 (1991).
- [2] K. Kimura, K. Ohshima, and M. Mannami, *Appl. Phys. Lett.* **64**, 2232 (1994).
- [3] M. Geretschlager, *Nucl. Instrum. Methods B* **204**, 479 (1983).
- [4] P. Bailey, T. C. Q. Noakes, C. J. Baddeley, S. P. Tear, and D. P. Woddruff, *Nucl. Instrum. Methods Phys. Res., Sect. B* **183**, 62 (2001).
- [5] Y. Kido, T. Nishimura, Y. Hoshino, and H. Namba, *Nucl. Instrum. Methods B* **161–163**, 371 (2000).
- [6] P. Sigmund, *ICRU News* **1**, 17 (2000).
- [7] N. R. Arista, K. Dan. Vidensk. Selsk. Mat. Fys. Medd. **52**, 595 (2006).
- [8] C. C. Montanari, J. E. Miraglia, and N. R. Arista, *Phys. Rev. A* **66**, 042902 (2002).
- [9] ASTAR: Stopping power and range tables for helium ions, available from <http://physics.nist.gov/PhysRefData/Star/Text/ASTAR.html>
- [10] PSTAR: Stopping power and range tables for protons, available from <http://physics.nist.gov/PhysRefData/Star/Text/PSTAR.html>
- [11] J. F. Ziegler, SRIM, available from: <http://www.srim.org/>
- [12] J. F. Ziegler, *Nucl. Instrum. Methods B* **219**, 1027 (2004).
- [13] P. Sigmund and A. Schinner, *Nucl. Instrum. Methods B* **195**, 64 (2002).
- [14] N. R. Arista and A. F. Lifschitz, in *Advances in Quantum Chemistry: Theory of the Interaction of Swift Ions with Matter, Part I*, edited by R. Cabrera-Trujillo and J. R. Sabin (Elsevier, Amsterdam, 2004), Vol. 45, p. 47.
- [15] G. Schiwietz and P. L. Grande, *Phys. Rev. A* **84**, 052703 (2011); CasP, available from http://www.helmholtz-berlin.de/people/gregor-schiwietz/casp_en.html
- [16] H. Paul, Stopping powers for light ions, available from <http://www.exphys.jku.at/stopping/>
- [17] E. Fermi and E. Teller, *Phys. Rev.* **72**, 399 (1947).
- [18] J. E. Valdes, J. C. Eckardt, G. H. Lantschner, and N. R. Arista, *Phys. Rev. A* **49**, 1083 (1994).
- [19] E. A. Figueroa, E. D. Cantero, J. C. Eckardt, G. H. Lantschner, J. E. Valdes, and N. R. Arista, *Phys. Rev. A* **75**, 010901 (2007).
- [20] S. N. Markin, D. Primetzhofer, M. Spitz, and P. Bauer, *Phys. Rev. B* **80**, 205105 (2009).
- [21] H. O. Funsten, S. M. Ritzau, R. W. Harper, J. E. Borovsky, and R. E. Johnson, *Phys. Rev. Lett.* **92**, 213201 (2004).
- [22] L. N. Serkovic, E. A. Sanchez, O. Grizzi, J. C. Eckardt, G. H. Lantschner, and N. R. Arista, *Phys. Rev. A* **76**, 040901 (2007).
- [23] S. N. Markin, D. Primetzhofer, and P. Bauer, *Phys. Rev. Lett.* **103**, 113201 (2009).
- [24] K. Eder, D. Semrad, P. Bauer, R. Golser, P. Maier-Komor, F. Aumayr, M. Pealbalba, A. Arnau, J. M. Ugalde, and P. M. Echenique, *Phys. Rev. Lett.* **79**, 4112 (1997).
- [25] J. I. Juaristi, C. Auth, H. Winter, A. Arnau, K. Eder, D. Semrad, F. Aumayr, P. Bauer, and P. M. Echenique, *Phys. Rev. Lett.* **84**, 2124 (2000).
- [26] S. P. Moller, A. Csete, T. Ichioka, H. Knudsen, U. I. Uggerhoj, and H. H. Andersen, *Phys. Rev. Lett.* **93**, 042502 (2004).
- [27] R. Golser and D. Semrad, *Phys. Rev. Lett.* **66**, 1831 (1991).
- [28] D. I. Thwaites, *Radiat. Res.* **95**, 495 (1983).
- [29] D. Primetzhofer, S. N. Markin, and P. Bauer, *Nucl. Instrum. Methods B* **269**, 2063 (2011).
- [30] R. C. Monreal, *Prog. Surf. Sci.* **89**, 80 (2014).
- [31] D. Primetzhofer, S. Rund, D. Goebel, D. Roth, and P. Bauer, *Phys. Rev. Lett.* **107**, 163201 (2011).
- [32] D. Primetzhofer, *Phys. Rev. B* **86**, 094102 (2012).
- [33] H. H. Brongersma, M. Draxler, M. de Ridder, and P. Bauer, *Surf. Sci. Rep.* **62**, 63 (2007).
- [34] P. Kuernsteiner, R. Steinberger, D. Primetzhofer, D. Goebel, T. Wagner, Z. Druckmuellerova, P. Zeppenfeld, and P. Bauer, *Surf. Sci.* **609**, 167 (2013).
- [35] T. V. Perevalov, V. A. Gritsenko, S. B. Erenburg, A. M. Badalyan, H. Wong, and C. W. Kim, *J. Appl. Phys.* **101**, 053701 (2007).
- [36] S. Suzer, S. Sayan, M. M. Banaszak Holl, E. Garfunkel, Z. Hussain, and N. M. Hamdan, *J. Vac. Sci. Technol. A* **21**, 106 (2003).
- [37] D. Primetzhofer, *Nucl. Instrum. Methods Phys. Res., Sect. B* **320**, 100 (2014).
- [38] Y. Hoshino, Y. Kido, K. Yamamoto, S. Hayashi, and M. Niwa, *Appl. Phys. Lett.* **81**, 2650 (2002).
- [39] K. Saskawa, K. Fujikawa, and T. Toyoda, *Appl. Surf. Sci.* **255**, 1551 (2008).
- [40] K. Nakajima, S. Joumori, M. Suzuki, K. Kimura, T. Osipowicz, K. L. Tok, J. Z. Zheng, A. See, and B. C. Zhang, *Appl. Surf. Sci.* **237**, 416 (2004).
- [41] H. S. Chang, H. Hwang, M. H. Cho, and D. W. Moon, *Appl. Phys. Lett.* **86**, 031906 (2005).
- [42] M. Behar, R. C. Fadanelli, I. Abril, R. Garcia-Molina, C. D. Denton, L. C. C. M. Nagamine, and N. R. Arista, *Phys. Rev. A* **80**, 062901 (2009).
- [43] J. A. Leavitt, L. C. McIntyre, M. D. Ashbaugh, J. G. Oder, Z. Lin, and B. Dezfouly-Arjomandy, *Nucl. Instrum. Methods B* **44**, 260 (1990).
- [44] D. Primetzhofer, E. Dentino Litta, A. Hallen, M. Linnarsson, and G. Possnert, *Nucl. Instrum. Methods Phys. Res., Sect. B* (to be published).
- [45] M. K. Linnarsson, A. Hallen, J. Astrom, D. Primetzhofer, S. Legendre, and G. Possnert, *Rev. Sci. Instrum.* **83**, 095107 (2012).
- [46] J. P. Biersack, E. Steinbauer, and P. Bauer, *Nucl. Instrum. Methods B* **61**, 77 (1991).
- [47] J. F. Ziegler, J. P. Biersack, and U. Littmark, *The Stopping and Range of Ions in Solids* (Pergamon, New York, 1985), Vol. 1.
- [48] G. Moliere, *Z. Naturforsch.* **A2**, 133 (1947).
- [49] W. K. Chu, *Phys. Rev. A* **13**, 2057 (1976).
- [50] N. P. Barradas, E. Alves, Z. Siketic, and I. Bogdanovic Radovic, in *Proceedings of the Twentieth International Conference on Application of Accelerators in Research and Industry*, edited by F. D. McDaniel and B. L. Doyle, AIP Conf. Proc. No. 1099 (AIP, Melville, NY, 2009), p. 331.
- [51] E. Dentoni Litta, P.-E. Hellstrom, C. Henkel, and M. Ostling, in *Proceedings of the 13th International Conference on Ultimate Integration on Silicon (ULIS)* (IEEE, New York, 2012), p. 105.
- [52] I. Abril, R. Garcia-Molina, C. D. Denton, F. J. Perez-Perez, and N. R. Arista, *Phys. Rev. A* **58**, 357 (1998).
- [53] S. Heredia-Avalos, R. Garcia-Molina, J. M. Fernandez-Varea, and I. Abril, *Phys. Rev. A* **72**, 052902 (2005).
- [54] P. Bauer, W. Rossler, and P. Mertens, *Nucl. Instrum. Methods Phys. Res., Sect. B* **69**, 46 (1992).
- [55] C. Pascual-Izarra, M. Bianconi, G. Lulli, and C. Summonte, *Nucl. Instrum. Methods Phys. Res., Sect. B* **196**, 209 (2002).
- [56] D. C. Santry and R. D. Werner, *Nucl. Instrum. Methods Phys. Res., Sect. B* **14**, 169 (1986).

- [57] W. N. Lennard, H. Xia, and J. K. Kim, *Nucl. Instrum. Methods Phys. Res., Sect. B* **215**, 297 (2004).
- [58] I. Nagy, A. Arnau, and P. M. Echenique, *Phys. Rev. A* **40**, 987 (1990).
- [59] E. A. Figueroa and N. R. Arista, *J. Phys.: Condens. Matter* **22**, 015602 (2010).
- [60] Y. Xu and W. Y. Ching, *Phys. Rev. B* **44**, 11048 (1991).
- [61] E. K. Chang, M. Rohlfing, and S. G. Louie, *Phys. Rev. Lett.* **85**, 2613 (2000).
- [62] D. Goebel, D. Roth, D. Primetzhofer, R. C. Monreal, A. Abad, and P. Bauer, *J. Phys.: Condens. Matter* **25**, 485006 (2013).